NRC Research Press

ARTICLE

Tree biomass reconstruction shows no lag in postglacial afforestation of eastern Canada

Olivier Blarquez and Julie C. Aleman

Abstract: Forest ecosystems in eastern Canada are particularly sensitive to climate change and may shift from carbon sinks to carbon sources in the coming decades. Understanding how forest biomass responded to past climate change is thus of crucial interest, but past biomass reconstruction still represents a challenge. Here we used transfer functions based on modern pollen assemblages and remotely sensed biomass estimation to reconstruct and quantify, for the last 14 000 years, tree biomass dynamics for the six main tree genera of the boreal and mixedwood forests (*Abies*, *Acer*, *Betula*, *Picea*, *Pinus*, *Populus*). We compared the mean genera and total biomass with climatic (summer temperatures and annual precipitation), physical (CO_2, insolation, ice area), and disturbance (burned biomass) variables to identify the potential drivers influencing the long-term trends in tree biomass. For most genera, tree biomass was related to summer temperature, insolation, and CO_2 levels; *Picea* was the exception and its biomass also correlated with annual precipitation. At the onset of the Holocene and during the Holocene Thermal Maximum (ca. 10 000–6000 BP), tree biomass tracked the melting of the Laurentide Ice Sheet with high values (>50 tonnes·ha^{-1} and a total of 12 Pg). These values, in the range of modern forest ecosystems biomass, indicate that trees were probably able to survive in a periglacial environment and to colonize the region without any discernible lag by tracking the ice retreat. High biomass at the beginning of the Holocene was likely favoured by higher than present insolation, CO_2 levels higher than during the Last Glacial Maximum, and temperature and precipitation close to present-day levels. Past tree biomass reconstruction thus brings novel insights about the drivers of postglacial tree biomass and the overall biogeography of the region since the deglaciation.

Key words: tree biomass, pollen, Last Glacial Maximum, Holocene, modern analogue technique, climate.

Résumé : Les écosystèmes forestiers de l'est du Canada sont particulièrement sensibles aux changements climatiques et pourraient passer de puits à source de carbone dans les décennies à venir. Il est par conséquent crucial de comprendre de quelle façon la biomasse forestière a réagi aux changements climatiques passés. Cependant, la reconstitution de la biomasse passée représente encore actuellement un défi. Dans cette étude, nous avons utilisé des fonctions de transfert développées à partir d'assemblages modernes de pollen et d'estimations de la biomasse arborée aérienne issues de la télédétection afin de reconstituer et quantifier, pour les 14 000 dernières années, la dynamique de la biomasse des six principaux genres d'arbres (*Abies*, *Acer*, *Betula*, *Picea*, *Pinus*, *Populus*) des forêts mixtes et boréales. Nous avons ainsi comparé la biomasse moyenne de chaque genre et la biomasse totale des six genres à des variables climatiques (températures estivales et précipitation annuelle), physiques (CO_2, insolation, étendue de glace) et en lien avec les perturbations (biomasse brûlée) afin d'identifier les facteurs potentiels qui influencent l'accumulation de biomasse à long terme. La biomasse des arbres était, chez la plupart des genres, reliée à la température estivale, au degré d'insolation et au niveau de CO_2; le genre *Picea* faisant exception, sa biomasse étant également corrélée aux précipitations annuelles. Au début de l'Holocène et durant le maximum thermique holocène (il y a environ 6000–10 000 ans), la biomasse des arbres a suivi la fonte de l'inlandsis laurentidien avec des valeurs élevées (>50 t·ha^{-1} et un total de 12 Pg). Ces valeurs, qui correspondent à celles de la biomasse des écosystèmes forestiers modernes, indiquent que les arbres étaient probablement capables de survivre dans un environnement périglaciaire et de coloniser la région sans aucun décalage en suivant le retrait de la glace. Les valeurs élevées de la biomasse forestière au début de l'Holocène ont vraisemblablement été favorisées par une insolation plus prononcée qu'actuellement, des niveaux de CO_2 plus élevés que durant le Dernier Maximum Glaciaire ainsi que des températures et des précipitations proches de l'actuel. La reconstruction de la biomasse passée des arbres apporte par conséquent de nouvelles informations concernant les facteurs qui ont influencé la construction de la biomasse forestière durant la période postglaciaire et sur la biogéographie générale de la région depuis la déglaciation.

Mots-clés : biomasse des arbres, pollen, Dernier Maximum Glaciaire, Holocène, technique des analogues modernes, climat.

1. Introduction

In eastern Canada, forests are particularly sensitive to climate change, and numerous factors may contribute to reversing their carbon sink capacity into a source such as, for example, increased disturbance frequency by fire (Mack et al. 2011) or biotic agents (Hicke et al. 2012), increased drought frequency (Ma et al. 2012), or increased permafrost thawing and the associated emissions from soil microorganisms at the forest–tundra ecotone (Schuur et al. 2009). For example, carbon emissions from fires in northern ecosystems, notably in tundra and boreal forest, represent a significant proportion of global emissions (Bradshaw et al. 2009). Reconstructing the temporal dynamics of forest biomass is crucial for understanding the processes that influence carbon storage and helping forecast forest responses to ongoing global changes.

Received 22 May 2015. Accepted 22 December 2015.

O. Blarquez. Department of Geography, Université de Montréal, Montréal, QC H3C 3J7, Canada.
J.C. Aleman. Department of Ecology and Evolutionary Biology, Yale University, New Haven, CT 06511, USA.
Corresponding author: Olivier Blarquez (email: blarquez@gmail.com).

Additionally, forest ecosystems are composed of long-lived organisms, and the mechanisms underlying their dynamics take place at a scale spanning centuries to millennia (e.g., forest succession, range expansions; Feurdean et al. 2013; Bergeron et al. 2004). To put into perspective the temporal dynamics of forest biomass regarding climate and natural forcing, vegetation reconstruction would gain by being performed at the millennial time scale. To date, the main source of information that could be used to infer past biomass comes from the analysis of bioproxies such as pollen (Seppä et al. 2009) or plant macroremains (Blarquez et al. 2012), extracted from sedimentary archives, or the analysis of historical vegetation surveys (Rhemtulla et al. 2009).

Transfer functions could be used to relate paleoecological proxies accumulation in sediments with environmental conditions (e.g., climate, pH, etc.) or community features (e.g., vegetation cover, biome type). Those functions are based on the principle that biological samples (e.g., pollen) with similar taxa composition were produced by plant communities with similar compositional and structural characteristics. Among those functions, the modern analog technique (MAT) is one of the most widely used in paleoecological studies (Overpeck and Webb 1985). In MAT, first, modern pollen assemblages are calibrated against modern vegetation features, then modern pollen samples are compared with fossil samples and the closest analogues based on compositional similarity are chosen, and finally, the fossil pollen samples are assigned the vegetation feature associated with its closest modern analogs. This technique has been successfully used to reconstruct tree cover in North America since the Last Glacial Maximum (LGM; 21 000 BP) with MAT calibrated using pollen assemblages and satellite tree cover measures (Williams 2002; Williams et al. 2011).

The calibration step generally involves the comparison of modern samples with standing vegetation by using land surveys (Seppä et al. 2009), trapping protocols (Blarquez et al. 2012), or remote-sensing data (Williams, 2002). Here the availability of quantified and homogeneous vegetation measures at the same spatial scale as modern pollen databases is crucial (Whitmore et al. 2005). Such data have recently become available for living-tree aboveground biomass covering Canada in the form of maps of specific tree biomass estimations at a 250 × 250 m resolution for a vegetation gradient that ranges from the temperate forest to the tundra (Beaudoin et al. 2014). Before relating pollen assemblages to modern biomass, certain precautions must be taken and assumptions must be made. Notably, the accumulation of pollen in sediments is affected by numerous taphonomical biases, including differential productivity and dispersal of taxa, as well as the spatial scale at which pollen are representative of the population actually producing them (Bradshaw and Webb 1985). These uncertainties are also associated with sedimentary archive type and characteristics such as the deposit environment, the basin size, the sediment accumulation rate, or the choice of an age–depth model. Here we used pollen relative abundances (i.e., percentage data) because they help standardize the data between variable sedimentary sites (Williams 2002). Pollen accumulation rates should allow for absolute estimates of pollen concentrations and so are superior in theory for reconstructing biomass (Seppä et al. 2009), but in practice, they are too sensitive to taphonomic biases and no modern pollen database expressed in accumulation rate is available (Whitmore et al. 2005).

Our objectives were thus to use MAT to relate modern tree biomass to modern pollen assemblages from Whitmore et al. (2005) and to compare modern and fossil pollen assemblages expressed in relative abundances for reconstructing the past biomass of ecosystems. We focused on eastern Canada (i.e., east of 100°W) because (*i*) the dominant tree forest species that span the area are replaced with nonanalogous western and mountain species west of 100°W (e.g., *Abies balsamea*, replaced with *Abies grandis* or *Abies lasiocarpa*), which would thus require a regional split of pollen types to ensure MAT accuracy (Williams and Shuman 2008), and (*ii*) because of the Canadian distribution of the calibration dataset (Beaudoin et al. 2014). These quantified data that we obtained are crucial to understanding the biogeography of the region and could provide useful information for models linking vegetation dynamics to climate and (or) disturbance. Finally, we compared tree biomass dynamics with climatic and physical variables to highlight the potential drivers of the afforestation process and evaluate its temporal variability.

2. Material and methods

2.1. Modern analogue technique

The modern pollen samples that have been used for constructing the transfer functions were selected from the North American Surface Sample Dataset (Fig. 1; Whitmore et al. 2005). Before the analysis, all samples were standardized to consider, at minimum, the genus level and the family level when necessary. For example, for certain taxa, when the determination level between analyses was not homogeneous enough for classification to the genus level, we aggregated those taxa at the family level (Williams and Shuman 2008). Fifty-three genera and 28 families were considered (Supplementary Table S1[1]).

We used MAT based on squared-chord distance (SCD) to establish transfer functions between modern pollen assemblages and tree biomass (Overpeck and Webb 1985). We used the tree biomass of the six forest tree genera that contributed the most to the total biomass above ca. 40°N, i.e., *Picea*, *Pinus*, and *Abies* for needle-leaved trees and *Acer*, *Betula*, and *Populus* for broadleaved trees. Those genera are representative of the Canadian boreal, mixed boreal, and Laurentian forests, and we limited our interpretation to those ecosystems. We used the biomass maps at 250 × 250 m resolution produced by Beaudoin et al. (2014) and based on a *k* nearest neighbour (*k*NN) approach and MODIS imagery. According to Beaudoin et al. (2014), biomass estimates error is greater in mountain regions, in low biomass areas, and in regions where calibration data (i.e., aerial photographs) for the *k*NN procedure are sparse. Those situations do not generally apply for modern pollen assemblage sites located in the boreal and temperate forests (Fig. 1), and the spatial aggregation of biomass pixel values to 1 km^2 and beyond for all sites (see below) likely improved biomass estimates accuracy (Beaudoin et al. 2014). To obtain genera biomass maps, we summed the biomass of several species: *Picea* represented the sum of *P. glauca* and *P. mariana*; *Pinus* represented that of *P. banksiana*, *P. strobus*, and *P. resinosa*, and *Abies* represented *Abies balsamea* solely. For broadleaved trees, *Acer* represented the sum of *A. rubrum*, *A. saccharum*, *A. saccharinum*, *A. pensylvanicum*, and *A. spicatum*; *Betula* represented that of *B. papyfera* and *B. alleghaniensis*, and finally *Populus* represented that of *P. tremuloides* and *P. balsamifera*. We selected the modern pollen samples located in Canada, east of 100°W (Fig. 1). To limit pollen taphonomy uncertainties related to spatial representation, we selected modern samples obtained solely from lacustrine environments, excluding, for example, moss polster and Tauber trap pollen samples.

Before calculating modern tree biomass estimated from remote sensing around modern pollen samples, we evaluated the optimal distance for extracting biomass values by replicating the MAT calibration step with increasing distances such as radius = 1, 5, 15, …, 150 km (Fig. 2). For each set of MAT replicates, we

[1]Supplementary data are available with the article through the journal Web site at http://nrcresearchpress.com/doi/suppl/10.1139/cjfr-2015-0201: cjfr-2015-0201suppla.pdf contains Supplementary Table S1 and Fig. S1; cjfr-2015-0201supplb.xlsx contains Supplementary Table S2.

Fig. 1. Present day biomass (in t·ha^{-1}) for the six studied genera ((*a*) *Abies*, (*b*) *Acer*, (*c*) *Betula*, (*d*) *Picea*, (*e*) *Pinus*, (*f*) *Populus*) from Beaudoin et al. (2014) and the location of modern pollen samples (grey dots) from the North American Surface Sample Dataset (Whitmore et al. 2005). The spatial resolution of the biomass raster has been reduced to 10 × 10 km compared with the original 250 × 250 m resolution for display purpose only. (This figure is available in colour online.)

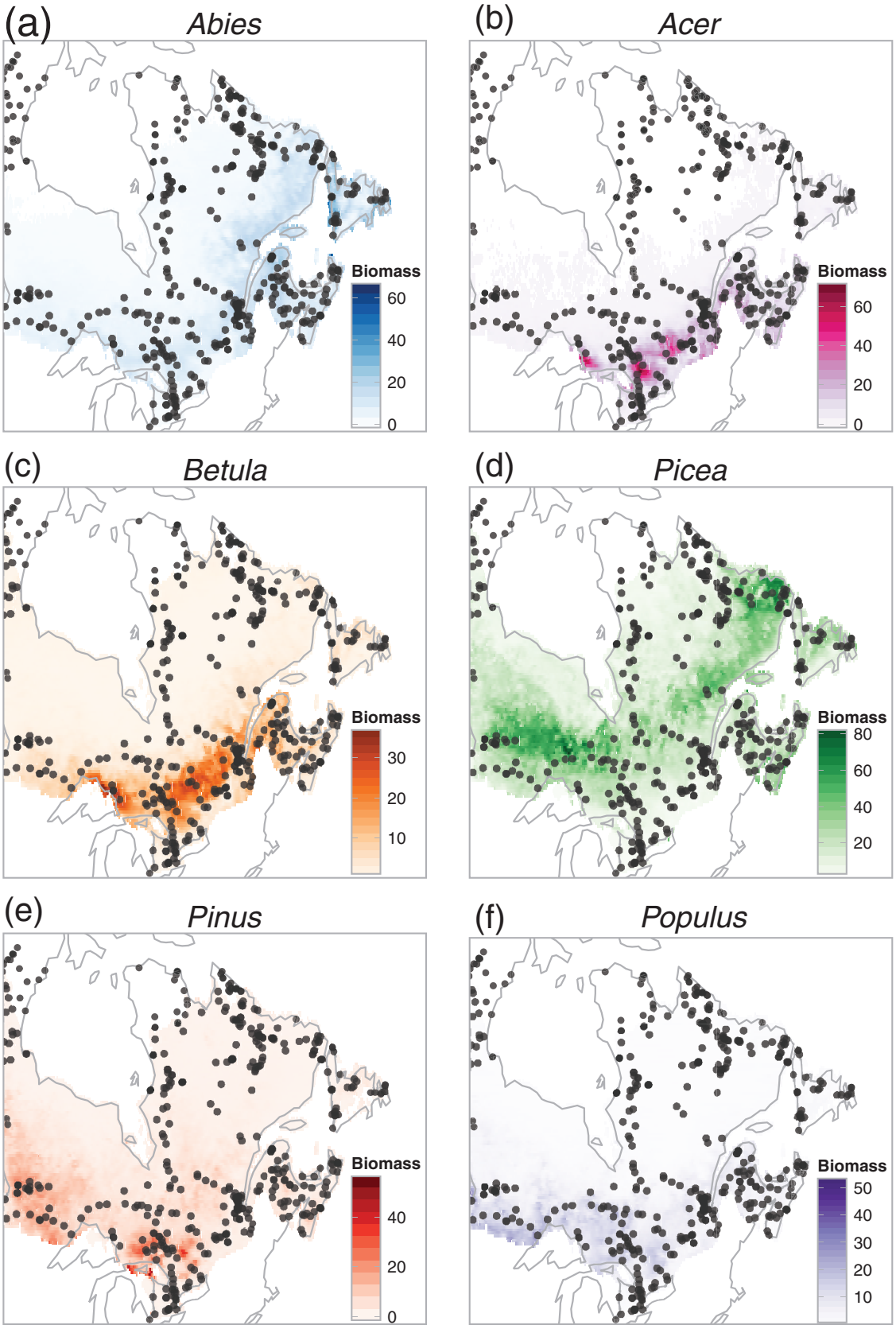

Fig. 2. Results from the procedure used to calculate the optimal radius for compiling the biomass around each sample of the modern pollen database for each genus, ((*a*) *Abies*, (*b*) *Acer*, (*c*) *Betula*, (*d*) *Picea*, (*e*) *Pinus*, (*f*) *Populus*) based on a compromise between high determination coefficient (r^2, dashed line), d(r^2) close or equal to 0 (solid lines), and a small distance. The selected distances are indicated for each genus on the graphs (grey dashed lines).

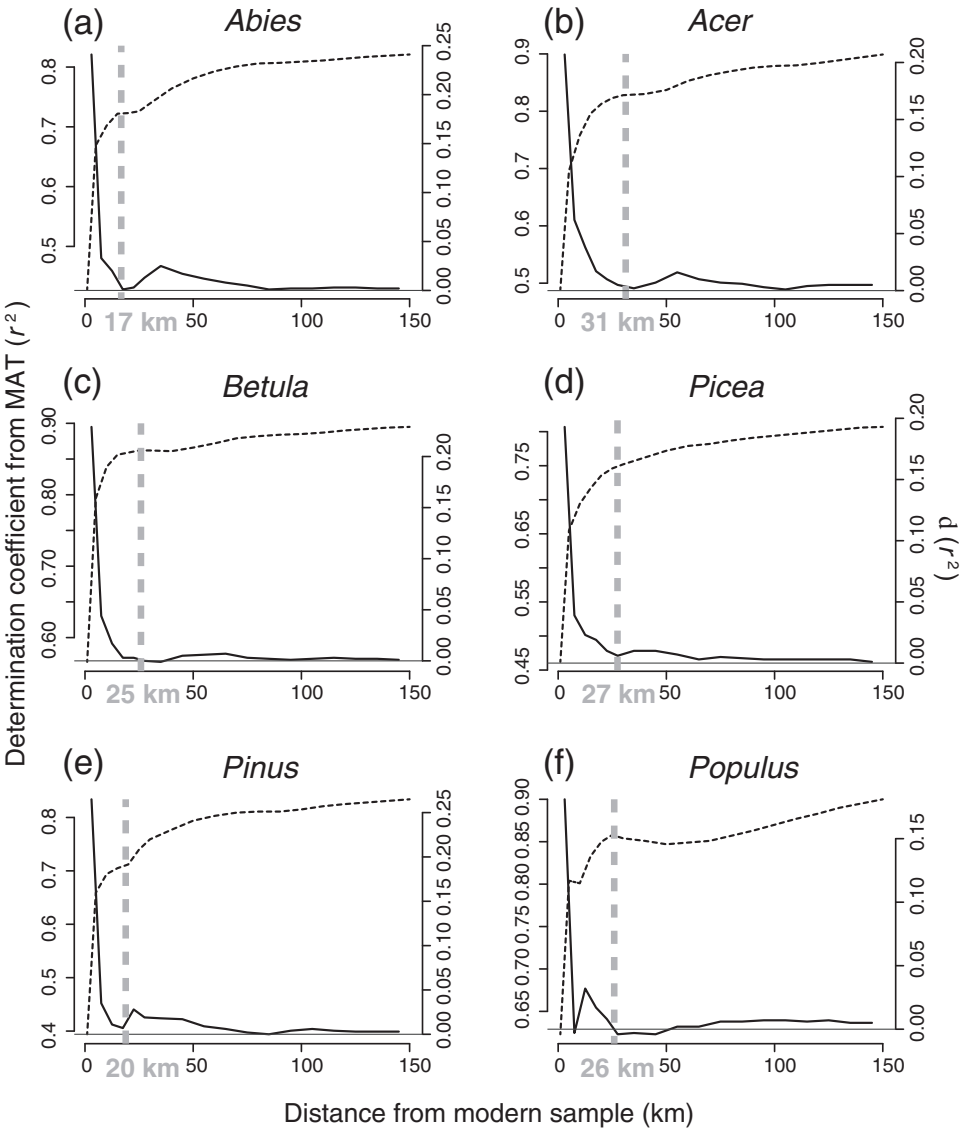

evaluated the leave-one-out cross-validation determination coefficient and its differential. The choice of an optimal distance was based on a compromise between high r^2, a small distance from the modern pollen sample, and an r^2 differential approaching or equal to 0, which indicates that increasing the radius did not significantly increase the MAT predictive power (Fig. 2).

We used these distances to compile the average biomass for each tree genus around each modern pollen sample. We evaluated the overall performance of the transfer functions by looking at predicted vs. observed biomass distribution, associated determination coefficients, and prediction uncertainty expressed by the root mean squared error of prediction (RMSEP; Fig. 3). The number of analogues needed to reconstruct past biomass (*k*) for each genus was evaluated by bootstrap resampling of the modern dataset, split into training and test sets (Simpson 2007). Although the choice of *k* is generally not strongly biased despite being determined post hoc from the training data, we used an independent optimization set alongside the usual training and test sets to avoid any bias in its choice (Telford et al. 2004). Before applying MAT, we used the receiver operating characteristic (ROC) curve approach (Gavin et al. 2003). Each sample in the modern dataset was assigned to a single vegetation zone according to Ramankutty and Foley (1999). The SCD between each sample and its *k*-closest analogues within each vegetation zone was compared with the *k*-closest SCDs from other vegetation zones. This approach enabled us to calculate the critical SCD value above which two samples cannot be selected as true analogues (Gavin et al. 2003). MAT transfer functions were then applied to fossil pollen assemblages extracted from the Neotoma Paleoecology Database (http://www.neotomadb.org) that were standardized to the same taxonomic levels that we used for the modern dataset (see Supplementary Table S1[1] for taxonomy and Supplementary Table S2[1] for the full citation list of the Neotoma sites; Grimm et al. 2013). We selected the pollen records (or sites) from the Neotoma Paleoecology Database that included at least one geochronological control point (i.e., ^{14}C or ^{210}Pb dating, tephra layer, etc.) for every 2500-year interval.

One hundred and fifty-two (152) sites were selected; the age–depth models of 133 were corrected according to the most up to date chronologies calculated by Blois et al. (2011). Eighteen sites, whose chronologies were expressed in radiocarbon years BP (^{14}C BP),

Fig. 3. Predicted vs. observed aboveground biomass for the six tree genera ((*a*) *Abies*, (*b*) *Acer*, (*c*) *Betula*, (*d*) *Picea*, (*e*) *Pinus*, (*f*) *Populus*) in eastern Canada. Determination coefficients, RMSEP, and the number of analogues used in the MAT for each genus are indicated on the graphs. Solid lines correspond to linear regressions applied to predicted vs. observed biomass (dashed lines represent 95% confidence intervals on linear regressions and dotted lines represent the prediction intervals).

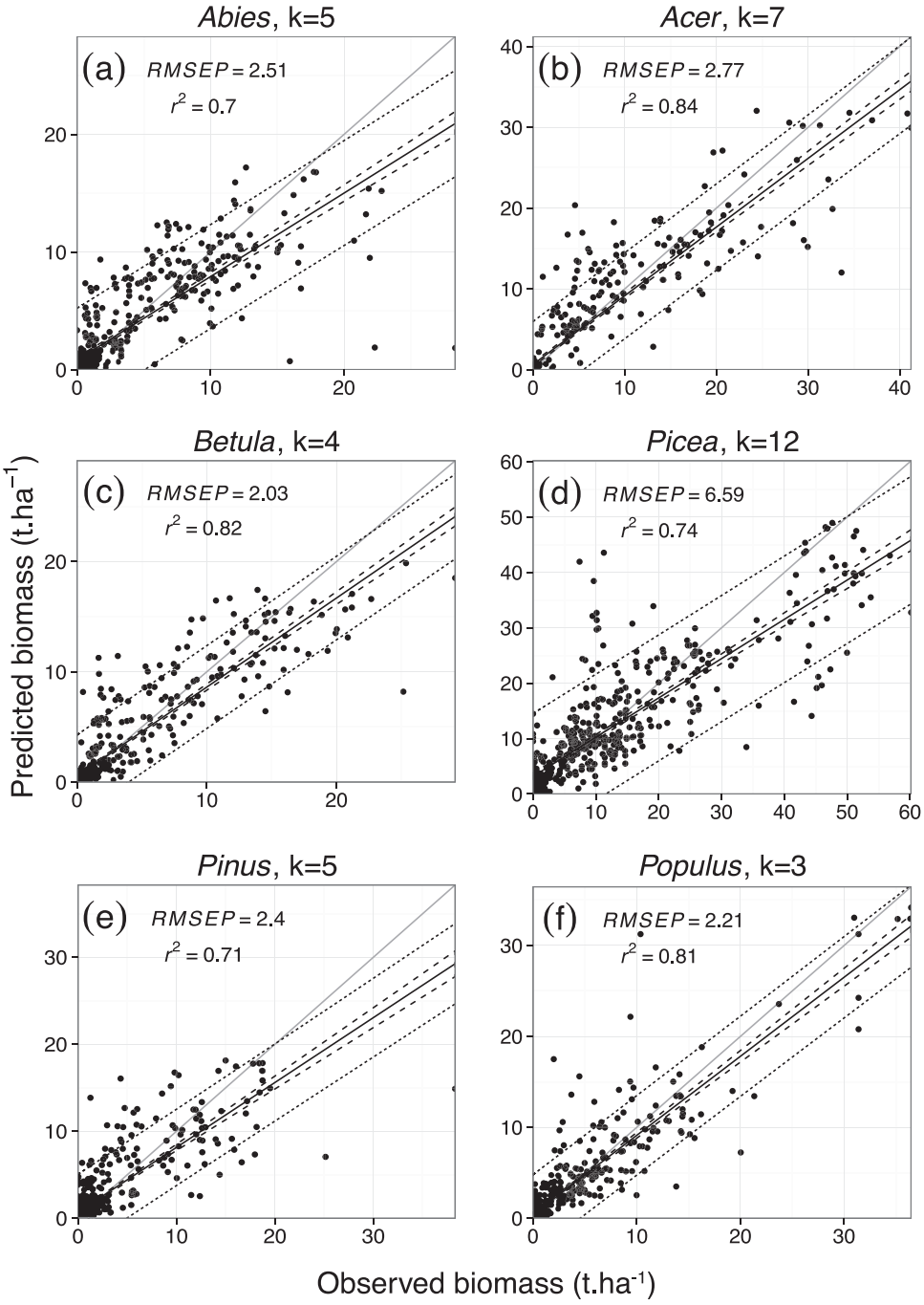

were converted to calibrated years (cal BP) using the IntCal13 calibration curve (Reimer et al. 2013) and the procedure developed by Grimm (2008). The chronology of one site, expressed in calibrated years BP, was left unmodified. Supplementary Table S2[1] lists the sites, the transformation applied in the age–depth models, the median time difference between original and corrected age–depth models, the location, and the original references for the datasets.

2.2. Biomass mapping

We used weighted spatiotemporal interpolation to produce gridded maps of reconstructed biomass values from selected pollen cores. A spatial grid of 50 km² pixels was used to interpolate biomass values for 1000-year intervals since 14 000 BP, i.e., ages = 14 000, 13 000, …, 0 BP. Spatial interpolation involved searching sites with biomass values located at a horizontal distance of 300 km and a vertical distance of 500 m from each grid cell centre. The temporal interpolation involved identifying biomass values within a temporal window of 500 years before and after each key date. Biomass values were then weighted using a tricube weighting function by considering their spatial distance to the grid centre and temporal distance to the key date. This

approach, which weights samples according to their spatio-temporal location, also downweights pollen sites (and thus reconstructed biomass values) that are poorly sampled (Williams et al. 2004). For each pixel, we used the weighted pollen biomass estimates to calculate the mean biomass per hectare (in tonnes (t)·ha^{-1}) for the six considered genera. We summed the values for those six genera to obtain the mean total biomass per pixel.

2.3. Climatic and physical variables

Laurentide Ice Sheet maps from Dyke (2004) were first calibrated to calendar ages (cal BP) using the IntCal13 (Reimer et al. 2013) calibration curves. Those maps were then used to constrain the biomass estimate maps and to compile the total area of the Laurentide Ice Sheet that was compared with the biomass values. We used paleoclimatic simulations from the HadCM3 general circulation model (GCM) (Singarayer and Valdes 2010) and from the CCSM3 GCM (Liu et al. 2009) obtained from http://ccr.aos.wisc.edu/resources/data_scripts/ to compare biomass dynamics with mean summer (June, July, and August) temperatures and mean annual precipitation anomalies. Those simulations consists of climatic averages at 1000-year intervals (i.e., maximum temporal resolution available) covering the last 14 000 years at a spatial resolution of 2.5° in latitude × 3.75° in longitude. For each experiment and each millennium interval, anomalies for air temperature (the difference between a given millennia and the pre-industrial (AD ca. 1750) period) and precipitation (the percentage of change between a given millennia and the pre-industrial period) were computed and downscaled using the CRU 3.10 and CRU 3.0 datasets for the HadCM3 and CCSM3, respectively. For each millennium, we compiled the mean anomalies of summer temperatures (in °C) and mean annual precipitation (in mm·day^{-1}) for pixels matching the biomass estimates maps and bootstrapped confidence intervals. We used the $\delta^{18}O$ of the North Greenland Ice Core Project (NGRIP) ice core record as an additional proxy for regional temperatures (Andersen et al. 2004), ice core CO_2 values from the Epica Dome C coring as a proxy of past CO_2 atmospheric content (Monnin et al. 2004), and insolation values at 45°N calculated using orbital parameters (Berger and Loutre 1991). For each millennium since 14 000 BP, we calculated the mean values of those proxies in 1000-year time windows (centred on millennia). Biomass burning trends were evaluated based on sedimentary charcoal composite curves. The approach is described in Blarquez et al. (2014*b*) and followed the data transformation explained in Power et al. (2008) involving a three-step transformation of charcoal data (min–max, Box–Cox, and *Z* score successive transformations). The compositing approach followed Daniau et al. (2012) and Marlon et al. (2013). The sites were obtained from the Global Charcoal Database (version 3; http://paleofire.org).

2.4. Statistical analyses

We used the biomass maps for each genus to calculate millennia mean and total biomass values. We summed millennia genus biomass values to obtain the total mean biomass value at each millennium. We used the least absolute shrinkage and selection operator (LASSO) regression method (Tibshirani 1996) to select climatic and physical variables that most strongly influence the total and each genus biomass dynamics. We used a 10-fold cross-validation approach to find the optimal λ value of the LASSO regression, which was then used to select the predictors of the model different from zero. Because the LASSO procedure is not invariant to linear transformations of the predictors, the physical and climatic variables were rescaled using *Z* scores prior to the analysis. This rescaling step further enabled us to rank and compare the predictors based on the value of their regression coefficients, a larger coefficient meaning that the predictor variable was more explanatory. The temporal trend in mean biomass was evaluated by fitting a LOWESS curve with a 200-year half-window width to the reconstructed biomass for all sites (Blarquez et al. 2014*b*, 2015).

3. Results

3.1. MAT accuracy

MAT was based on a set of 594 modern pollen samples distributed over Canada east of 100°W. The distance that best satisfied the compromise between high r^2, a small distance from the modern pollen sample, and an r^2 differential approaching or equal to 0 were 17 km for *Abies*, 31 km for *Acer*, 25 km for *Betula*, 27 km for *Picea*, 20 km for *Pinus*, and 26 km for *Populus*. For *Populus*, although d(r^2) was 0 at ca. 10 km, the 26 km distance significantly increased r^2. These distances are consistent with empirical studies of pollen source area (Bradshaw and Webb 1985) but are much higher compared with those of Sugita (1994), notably for *Abies*. However, we must consider that those distances are not representative of the direct relationship between a particular taxa and its landscape biomass but rather involve pollen assemblage relationships with genus landscape biomass expressed through MAT, which largely explains those longer distances. These distances are, however, in agreement with studies aimed at relating remotely sensed woody cover with pollen assemblages (Williams 2002). The examination of predicted vs. observed reconstructed biomass for each genus provides a coherent pattern indicating that the biomass values were well modelled (Fig. 3). For most genera, the error between modelled and observed biomass was inferior to 5 t·ha^{-1}, but the error was inherently higher for *Picea* due to its high biomass values notably in the boreal coniferous forests (Fig. 1). Additionally, maps comparing biomass predicted using MAT and fossil pollen samples from the 1900–2010 period and current biomass showed that the error could be important in areas that have experienced large anthropogenic influence during the last century (for example, in the St. Lawrence valley for *Acer* or *Betula*; Supplementary Fig. S1[1]). MAT determination coefficients were always above 0.5, and the RMSEP was below 3 t·ha^{-1} for most genera. This indicates that the reconstructions are accurate enough for reconstructing general tendencies of biomass dynamics at large spatial and temporal (millennia) scales. The number of analogues chosen by the optimization procedure ranged from 3 for *Populus* to 12 for *Picea* (Fig. 3). The best prediction was for *Betula*, which showed both a high determination coefficient (0.82) and a low RMSEP (2.03 t·ha^{-1}). For *Picea*, the RMSEP was high, with a value of 6.88 t·ha^{-1}, suggesting less certain reconstruction, but this value must be compared with the overall biomass range of the genus (0–60 t·ha^{-1}), which was almost twice that of all of the other genera. For all of the genera, the MAT tends to underestimate biomass values when observed biomass was above ca. 10 t·ha^{-1} (Fig. 3). The SCD critical value obtained from the ROC curve approach above which samples cannot be selected as true analogues was 0.14 SCD units. This value resulted in the exclusion of samples without analogues in the modern dataset mainly during the period before 10 000 BP, when the number of samples without analogues was as high as 50% (Fig. 4). After 10 000 BP and during the Holocene, this number stayed below 25% (Fig. 4).

3.2. Spatial biomass dynamics

Before 14 000 BP, the number of pollen sites was not sufficient enough for tree biomass reconstruction due to the presence of the Laurentide Ice Sheet (Fig. 4). After 14 000 BP, isolated sites began to accumulate sediments and thus pollen, enabling the reconstruction of biomass using MAT and the production of interpolated maps with more confidence since ca. 10 000 BP (Fig. 4). Generally, pollen core locations are well distributed across the territory, and by using the spatial weighting procedure, it was possible to produce maps covering the entire territory (excluding the northwestern area corresponding to northern Ontario and eastern Manitoba, where no pollen cores were available).

Fig. 4. Diagnostic plots for the MAT. (*a*–*d*) Location of the records from the Neotoma Paleoecology Database used to reconstruct the past biomass at 12 000, 8000, 4000, and 0 BP. (*e*) Total number of samples available within each 1000-year time interval from 14 000 to 0 BP. (*f*) Percentage of samples without analogue in the modern database within each 1000-year time interval, i.e., samples excluded by the ROC curve approach (Gavin et al. 2003).

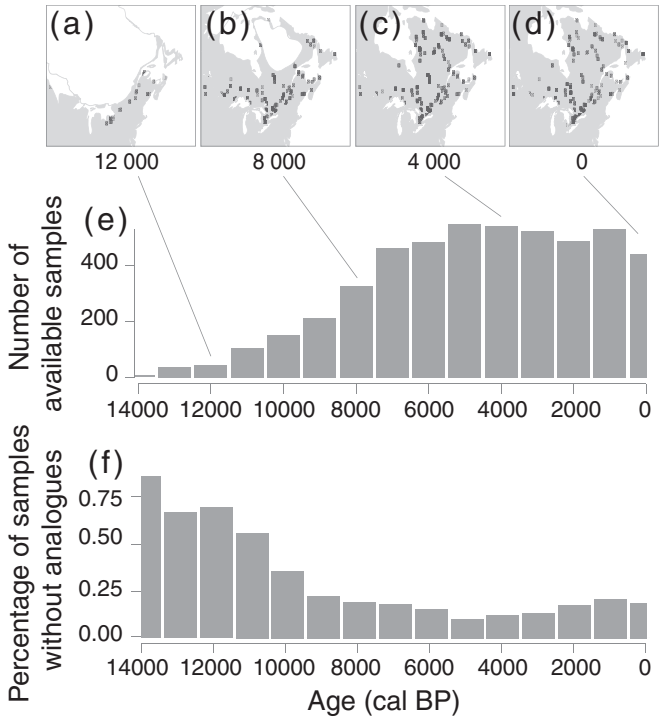

After 13 000 BP, *Picea* biomass increased up to its maximal level (with values above 19 t·ha^{-1}) in the direct vicinity of the ice sheet (Fig. 5). Before 11 000 BP, hotspots of *Picea* biomass were located east of the Great Lakes, but the overall area supported high *Picea* biomass with spatially continuous values above 11 t·ha^{-1}. At 9000 BP, a biomass hotspot was located between Lake Agassiz and Lake Objiway. After proglacial lakes disappeared, this hotspot tracked the melting of the remaining ice sheet eastward. From 5000 BP to 1000 BP, the biomass values for *Picea* were high across the region, with two notable centres of very high values located (*i*) east of Lake Winnipeg in Manitoba and western Ontario and (*ii*) in the Quebec Côte-Nord region and southern Labrador.

Before the Holocene period (starting ca. 11 700 BP), *Abies* biomass values were low, below 5 t·ha^{-1} (Fig. 5). Then, at the period centred around 11 000 BP (11 500 – 10 500 BP) *Abies* biomass started to increase, following a westward route from Nova Scotia, where high biomass values were recorded (between 8 and 29 t·ha^{-1}). During the Holocene, the area that displayed the highest values of *Abies* biomass remained spatially constant and localized in the northern part of the St. Lawrence region, Quebec Côte-Nord region, and the Canadian Maritime Provinces (New Brunswick, Nova Scotia).

High *Pinus* biomass values started to be recorded at 10 000 BP in an area that is bounded in the north by the proglacial Lakes Agassiz and Objiway and in the south by the Great Lakes. To the present day, the spatial distribution of the *Pinus* biomass has been characterized by high values (>7 t·ha^{-1}) located in southwestern Ontario and Manitoba (Fig. 5). The most notable *Pinus* biomass features were the westward expansion between 12 000 and 10 000 BP and a shrinking of its spatial distribution since 8000 BP that accelerated from 3000 BP (Fig. 5).

The spatial distribution of *Betula* biomass was largely similar to that of *Abies*. However, the localization of high *Betula* biomass values (>11 t·ha^{-1}) was generally limited to east of the St. Lawrence River and never spanned Newfoundland (Fig. 5).

The spatial pattern of *Populus* biomass was marked by a westward expansion since 13 000 BP. This expansion peaked at 8000 BP (Fig. 5). During the 8000 BP period, particularly high *Populus* biomass values (from 9 to 35 t·ha^{-1}) were found north of the Great Lakes in the area left by the draining of Lakes Agassiz and Objiway. *Populus* also expanded in the east (east of the St. Laurence River, Nova Scotia, and New Brunswick) after 9000 BP, but high biomass values disappeared from that area after 6000 BP. After that period and to the present day, the area of high *Populus* biomass shrank and remained located west of the St. Lawrence River, with a smaller area displaying high values located in Ontario and Manitoba between Lake Nigipon and Lake Winnipeg (Fig. 5).

Acer biomass values became high (i.e., between 12 and 42 t·ha^{-1}) only after 8000 BP, mainly east of the St. Lawrence region in areas that correspond to the current New Brunswick, Nova Scotia, and Quebec's Gaspé Peninsula. *Acer* spatial distribution then remained relatively constant and confounded with its present day distribution. For *Acer* but also for *Betula*, during the last 500 years, we observed a shrinking in their eastern distribution with a decrease of their biomass east of the St. Lawrence River and in the Maritimes Provinces.

The overall total biomass, i.e., the pixel sum of the six studied genera, started to increase, with very high values at approximately 10 000 – 9000 BP, in an area that corresponds to the current Maritime Provinces and Quebec (Fig. 5). Then areas of high biomass (>50 t·ha^{-1}) spanned north of the Great Lakes at 8000 BP mainly because of *Populus* and *Pinus* expansion. After 8000 BP, a contiguous belt of high biomass values (>ca. 43 t·ha^{-1}) matched the spatial distribution of the current boreal and boreal mixedwood forests. This area was split at its centre in an area that corresponds to south-central Quebec, favoured by the highly defined east–west pattern for the studied genera (east distribution for *Acer*, *Betula*, and *Abies* and west distribution for *Pinus* and *Populus*; Fig. 5).

3.3. Ranking the influence of physical and climatic processes

Summer insolation, GCM simulated summer temperatures, and atmospheric CO_2 content were the variables that had the strongest correlation to the total mean tree biomass (Fig. 6; Table 1). The total mean biomass was maximal during the period corresponding to the Holocene Thermal Maximum (HTM; ca. 10 000 – 6000 BP Kaufman et al. 2004). The LASSO procedure indicated that the genera dynamics followed this general pattern, i.e., a millennial dependence upon climatic condition (temperatures), solar energy expressed by insolation, and a positive relationship with the atmospheric CO_2 content. All genera appeared to be positively influenced by summer insolation and temperatures (expressed by NGRIP $\delta^{18}O$ or simulated by GCMs), especially *Pinus*. *Picea* biomass appeared to also depend on annual precipitation, contrary to the other genera for which precipitation did not appear to be limiting or that expressed a negative relationship to precipitation. The relationship of *Picea* to temperatures is unclear: it has a negative coefficient with $\delta^{18}O$ and a positive one with summer simulated temperature (Fig. 6; Table 1). Biomass burning appears related to only *Picea* and *Abies*, but this variable always has low coefficients compared with the other variables (Table 1).

4. Discussion

4.1. The spatiotemporal pattern of postglacial biomass construction and its drivers

The reconstructed spatiotemporal pattern of *Picea* biomass dynamics was coherent regarding the known history of the genus

Fig. 5. Biomass maps for the six genera and total biomass for the last 13 000 years and for present day (*k*NN MODIS; Beaudoin et al. 2014). The millennium period centered on 14 000 BP has not been mapped due to the low number of sites available for the mapping procedure. Color ranges have been defined by binning biomass values within five equal bins each representing 20% of the data (except for *Acer*, which were quartiles, i.e., 25% have been used for clarity). For an overview of all periods and to download the data (georeferenced raster tif files), refer to the online interactive application available at http://blarquez.com/maps. (This figure is available in colour online.) Figure 5 is concluded on next page.

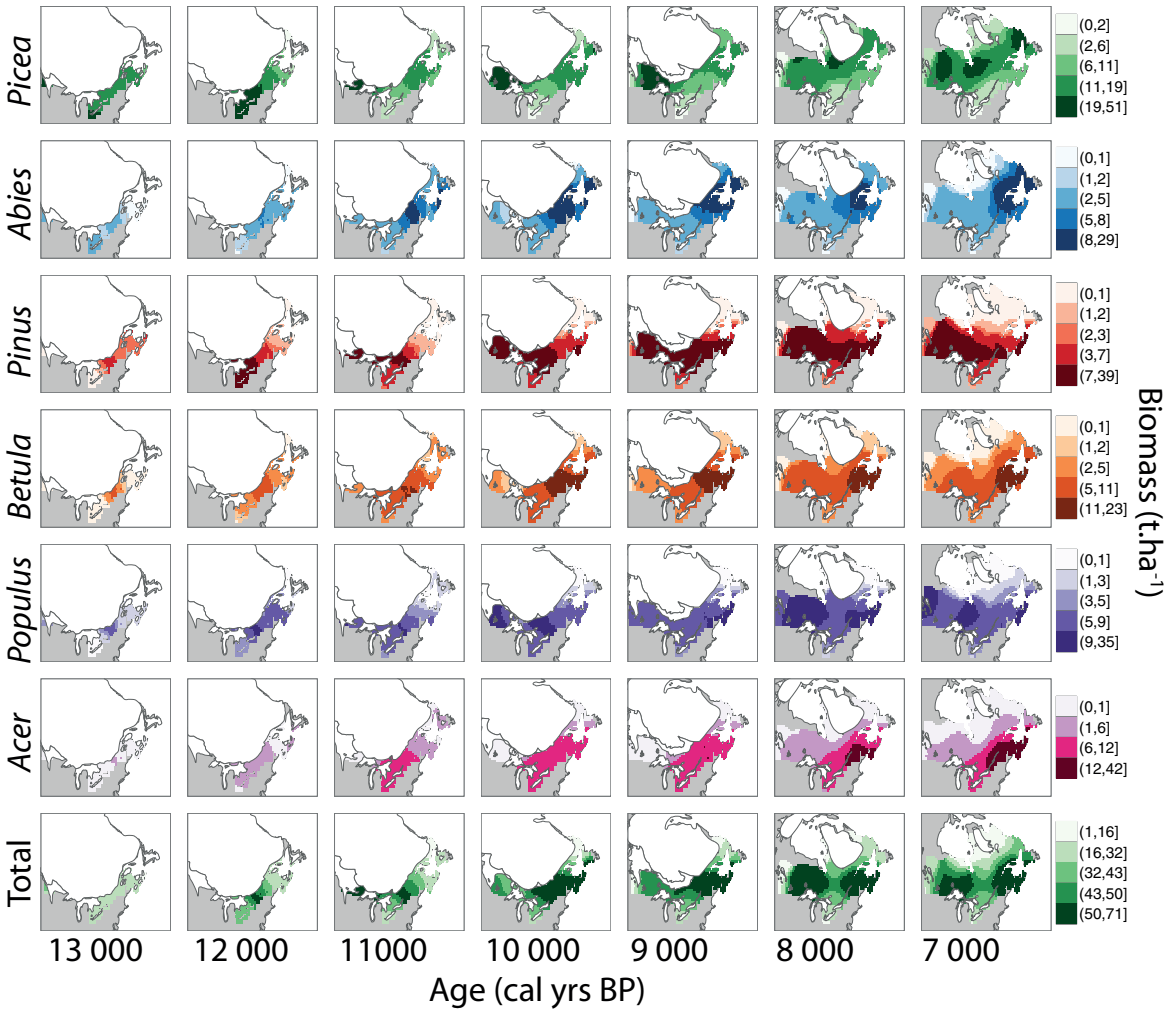

and its current status, particularly *Picea mariana*, which represents the highest contributor to the genus' biomass in the boreal forests. Moreover, this genus is the most abundant in the studied region, which corresponds to the boreal and mixedwood forests, at least since the LGM. Interestingly, the event known as the *Picea* decline that is supposed to span between 11 000 BP and 9000 BP is not apparent from our reconstructions (Figs. 5 and 6). Blois et al. (2011) precisely dated this *Picea* decline, by Bayesian change-point analysis, as around 11 500 BP and 10 100 BP from southern to northern Canadian sites, respectively. Although we cannot rule out *Picea* decline from occurring in eastern Canada, we can suspect that its decrease in pollen percentage may be the result of the proportional increase in other trees, notably broadleaved trees that expanded their biomass during the early Holocene (Fig. 6). Watts (1979) showed that the *Picea* pollen decline was not accompanied by a decline in *Picea* needle macrofossils and was thus likely a statistical artefact due to higher *Pinus* pollen production. It is then unsurprising that uncalibrated bioproxy dynamics may be misleading, even showing opposite trends when calibrated and expressed in quantified units (Blarquez et al. 2012; Marquer et al. 2014).

The mean biomass of the two other conifer genera, *Abies* and *Pinus*, followed a linear increase from 14 000 to 11 000 BP. During the HTM, both their mean biomass and spatial extent were maximal, potentially favoured by climatic conditions (temperatures and insolation; Table 1). This agrees with previous evidence suggesting that *Pinus*, notably *P. banksiana* and *P. resinosa*, was more abundant during the early Holocene period (before 7000 BP; Fuller 1997; Liu 1990). The spatial pattern of *Pinus* biomass clearly showed a westward expansion of the high biomass areas that were previously located in areas filled with the proglacial lakes. The temporal pattern of this expansion is thus coherent with the *Pinus* decline observed across southern Ontario (Fuller 1997; Liu 1990) and in the clay belt (Carcaillet et al. 2001).

Betula has been abundant since at least the beginning of the Holocene period over all of the territory. The areas of high abundance spanned south of the boreal mixedwood forest up to the closed boreal forests, probably corresponding to the ranges of *B. alleghaniensis* in the south and *B. papyfera* in the north. Interestingly, very high biomass values were recorded since 9000 BP east of the St. Lawrence River (>10 $t \cdot ha^{-1}$) that persisted until the last 500 years. Because *Betula* is a large pollen producer, little evidence

Fig. 5 (*concluded*). (This figure is available in colour online.)

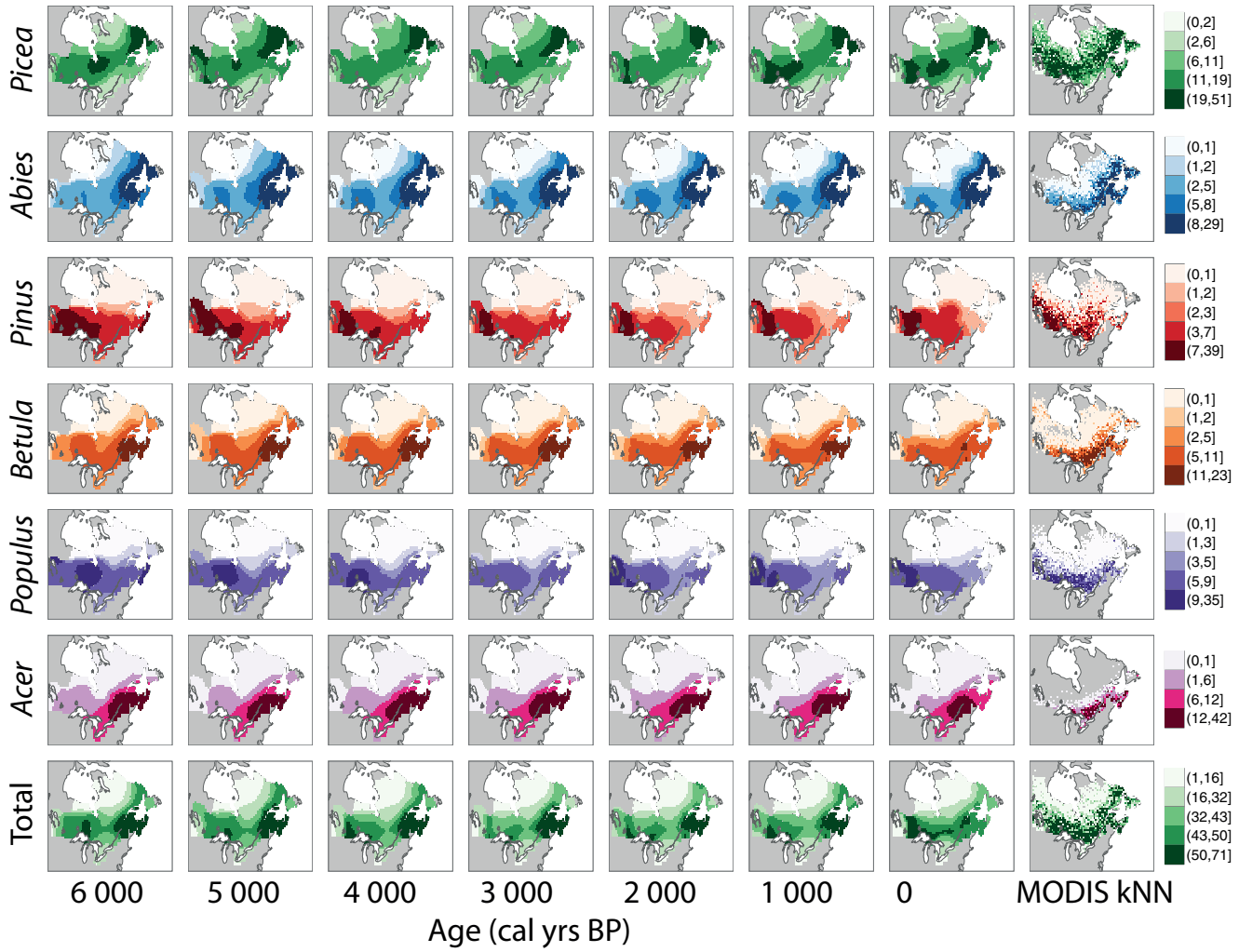

suggests any decline in the last 500 years and this genus should be compared with other large pollen producers (e.g., *Pinus*) to understand its biomass dynamics. For instance, based on pollen equatorial diameter, Asnong and Richard (2003) concluded that *B. alleghaniensis* was present in the Gaspé region during the mid-Holocene period and that both *Betula* tree genera (*B. alleghaniensis* and *B. papyfera*) then declined in favour of conifers (mainly *Picea* and *Abies*) during the last millennia. This process matches the observed biomass decrease in the eastern regions but the conifer increase was not apparent from the biomass reconstructions.

Contrary to *Betula*, *Populus* pollen is known to be poorly preserved in fossil records, making it difficult to absolutely quantify its presence in the past landscapes. *Populus* genus gathers pioneer trees (*P. tremuloides* and *P. balsamifera*) that produces large quantities of seeds, forms large clone colonies, and germinates on bare mineral soils. It has been shown that *P. tremuloides* growth is favored by higher June temperatures and a low thickness of the soil organic layer (Gewehr et al. 2014). Between 9000 BP and 8000 BP, the ice front continued to recede northwards, Lake Ojibway and Lake Agassiz drained (resulting in the 8200 cal BP climatic event) and a large lake bed containing glaciolacustrine deposits of sands, silts, and clays remained, thus creating favourable conditions for the invasion and growth of *Populus*, i.e., bare grounds and climatic conditions characteristic of the HTM (Fig. 6). Then, during the 8000 BP period, *Populus* attained its maximal spatial coverage and biomass with values up to ca. 35 t·ha^{-1} (Figs. 5 and 6). This result is in agreement with Comtois and Payette (1984), who concluded that the forest development phase in southern Quebec was accompanied by *Populus*, but these authors suggested the presence of open landscapes, in opposition to our biomass reconstruction that shows values above ca. 50 t·ha^{-1} as early as 10 000 BP (Fig. 5). These values are characteristic of forests and close to the current estimates for the boreal forest obtained from allometric equations (41.8 ± 2 t·ha^{-1}; Botkin and Simpson 1990) or remote-sensing data (73 t·ha^{-1}; Ranson et al. 1997). Growing evidence suggests that trees were able to survive and grow in periglacial conditions, i.e., directly at the proximity of glaciers, during the last glaciation in central Canada (Bélanger et al. 2014), in Alaska (Brubaker et al. 2005), or in Scandinavia (Kullman 2002). Moreover, the existence of an initial treeless tundra between the last deglaciation and the invasion of trees is still controversial (Liu 1990). Macrofossil evidence has suggested the local presence of trees at the ice margin as early as 12 000 BP (Jackson et al. 1997), and some pollen studies indicated that the proximity of ice did not necessarily support tundra-like vegetation, but rather forests, at the onset of the deglaciation (Richard et al. 1982). We do not rule out the presence of transient tundra-like vegetation before 10 000 BP that was interpreted from numerous pollen records (Ritchie 2004). Those tundra-like plant communities were characterised by a higher diversity (Blarquez et al. 2014b), contained assemblages without analogues in the modern dataset (Williams and Jackson 2007), and so were seemingly excluded by the ROC screening in our analysis (Fig. 4). This would eventually account for overinflating the mean biomass before 10 000 BP, but including no-analogue samples in

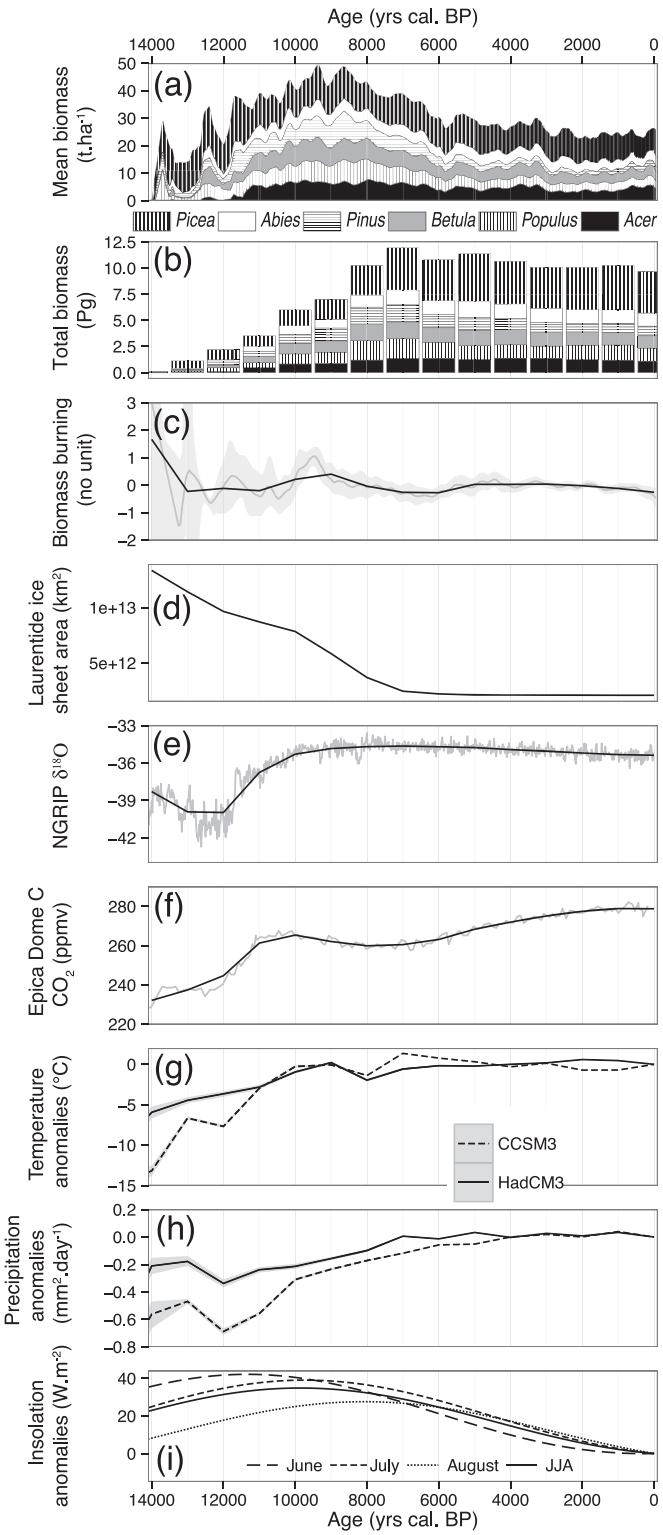

Fig. 6. Temporal trends of mean genera biomass compared with climatic and physical variables. (*a*) Mean tree genera biomass temporal trends obtained by fitting a LOWESS (with a 200-year half-window width) on reconstructed biomass from all sites. (*b*) Total biomass in 1000-year windows obtained by calculating the total biomass for each genera in each 50 km² pixel and then summing all pixel values within the studied territory. Total biomass values were expressed as petagrams (Pg) for convenience. (*c*) Biomass burning obtained by the analysis of charcoal series contained in the Global Charcoal Database (grey line) and 95% confidence interval (grey shaded area) and trend evaluated using 1000-year window averages (black line). (*d*) Laurentide Ice Sheet area trend from Dyke (2004). (*e*) NGRIP $\delta^{18}O$ record (grey line) and trend evaluated using 1000-year window averages (black line). (*f*) Epica Dome C CO_2 (grey line) from Monnin et al. (2004) and trend evaluated using 1000-year window averages (black line). Summer (JJA; June, July, August) (*g*) temperature and (*h*) annual precipitation anomalies from the HadCM3 and CCSM3 GCM experiments and 95% confidence interval (grey shaded area). (*i*) Summer (JJA) insolation anomalies at 45°N.

the reconstruction did not result in a lowering of mean biomass (results not shown; Fig. 6). Then, the existence of tree populations at the ice margin likely explains why biomass construction tracked the ice retreat and saturated so quickly. This hypothesis is among the only to also explain Reid's paradox, i.e., why postglacial tree migration rates are generally found to be faster compared with tree dispersal capacities (Feurdean et al. 2013).

The only genus whose biomass increase and postglacial migration appeared to be delayed is *Acer*. The increase in *Acer* biomass really began only during the Holocene and particularly after 6000 BP when populations of *A. saccharum* expanded in the eastern regions (Muller and Richard 2001) (Fig. 5). After this colonization phase, *Acer* became the second most important taxa in terms of biomass, reaching values up to 42 t·ha^{-1} (Fig. 6). This biomass pattern is in agreement with the results of Muller and Richard (2001), which indicated that the dominance of *Acer* in southern Quebec resulted from a dominance shift and, thus, from competition processes rather than from a migratory invasion.

Total tree biomass attained values ranging between 50 and 70 t·ha^{-1} as early as the beginning of the Holocene period in areas located in the direct vicinity of the ice margins (Fig. 5). Maximum genera biomass was attained during the HTM probably because of favorable climatic conditions but likely mainly because of higher than present insolation that led to higher energy released to the ground, which was then available for photosynthesis and tree growth. During the HTM, CO_2 levels were comparable with the Holocene long-term trend (>250 ppmv) and thus not likely to limit biomass construction for most genera (Fig. 6; Gerhart and Ward 2010). The interplay between CO_2 and vegetation is not trivial, however, particularly during the LGM when low CO_2 may have had strong physiological effects (Gerhart and Ward 2010) and at the beginning of the Holocene, because fires in the boreal region (whose fuel are dependent upon vegetation biomass; Blarquez and Carcaillet 2010) may have induced the postglacial increase in CO_2 levels (Carcaillet et al. 2002).

Our results may have strong implications for understanding how tree biomass may respond to ongoing climate change. For example, the most pessimistic "representative concentration pathway" developed by the IPCC, RCP 8.5, is predicting an increase of CO_2 up to 1300 ppm and a temperature increase of 4 °C by 2100 (van Vuuren et al. 2011). CO_2 fertilization may contribute to increased tree growth rate (Mousseau and Saugier 1992) and water efficiency (Keenan et al. 2013) and, therefore, would stimulate forest productivity and a higher tree biomass compared with present day. Higher temperature can also increase forest productivity, as happened during the HTM, but its role can be offset by the CO_2 increase that would hence stabilize growth rates (Tjoelker et al. 1998). Other factors such as natural and anthropogenic disturbances may compensate for potential increases in tree biomass. Fire frequency is projected to increase in the future decades (Flannigan et al. 2005), as will pest outbreaks (Dale et al. 2001), such that those disturbances by consuming biomass may offset the biomass increase stimulated by favourable climatic conditions. Potentially, species would tend to extend their northern range to track the warming, but it is not yet certain that boreal and temperate tree species will attain the migration rates

Table 1. Summary of the LASSO analysis to model mean tree biomass for the main genera and the mean total biomass against environmental variables.

	Abies	*Acer*	*Betula*	*Picea*	*Pinus*	*Populus*	Total
Intercept	—	—	—	—	—	—	—
Biomass burning	–0.062	—	—	0.541	—	—	—
JJA insolation	0.743	0.678	0.928	1.12	0.714	0.523	0.878
Ice area	0.195	0.194	—	–1.282	—	—	—
δ^{18}O NGRIP	–0.011	0.409	0.142	–2.988	0.35	0.343	—
JJA temperature	0.302	—	—	1.008	—	—	0.224
Annual precipitation	–0.131	–0.054	–0.294	0.935	—	—	—
CO_2	1.104	0.996	1.132	0.645	—	—	0.704

Note: Regression coefficients for the variables that have been selected by the LASSO regularization method used for model selection are shown. Dash "—" indicates variables not selected by the model. Prior to analysis variable have been rescaled using *Z* score to enable comparing the regression coefficients. JJA (summer: June, July, and August) temperature and annual precipitation were expressed as the mean of the HadCM3 and CCSM3 model runs. NGRIP, North Greenland Ice Core Project (NGRIP).

required to cope with climatic changes (Loarie et al. 2009). Indeed few evidences suggest northward migration of trees in eastern Canada (Caccianiga and Payette 2006). Moreover, the environmental conditions that these species would meet by extending their range are unknown, notably the fire–vegetation feedback (Girardin et al. 2013), as well as the potential resilience of ecosystems under no-analogue climates (Williams and Jackson 2007; Gauthier et al. 2015). Likewise, wood production and management in the commercial forests must be taken into account when predicting future biomass and ecosystem resilience to global changes (Gauthier et al. 2015).

The LASSO procedure results should generally be taken with caution to inform about the general temporal trends in biomass and its relationship to explaining factors, because we must assume that the role of temperature, precipitation, insolation, or CO_2 has varied through time and space. Moreover, we found that insolation and CO_2 were the best predictors of biomass trends, while the role of temperature is less clear. This can be a surprising result that may be explained by the differences among proxy uncertainty. Indeed, both insolation and CO_2 are estimated precisely from orbital parameters or ice cores, but the temperature and precipitation data are simulated using general circulation models, which can be the source of inaccuracies. Thus, temperature and precipitation may have played more important roles in biomass construction than highlighted by the regression model alone (Table 1). Interestingly, biomass burning trend such as expressed by the charcoal composite curve is always a poor predictor of tree biomass. The few weak relationships that have been found concerned conifers, for example, a positive one with *Picea* that is generally known to fuel fires (Johnson 1992) and a negative one with *Abies* and thus *A. balsamea* that is known for being the boreal conifer the least adapted to fire (Table 1). It has been shown that biomass burning is mostly a result of vegetation features through fuel buildup and that the relationship between biomass burning and vegetation tends to vary in space, being highly regionalized (Blarquez et al. 2015). The relationship between fire and vegetation was strongest in areas where dominance shifts between fuel types occurred (e.g., the boreal mixedwood forests; Higuera et al. 2009; Girardin et al. 2013; Blarquez et al. 2015). Consequently, the relationship between biomass burning and vegetation biomass cannot here be assessed beyond any doubt because of the inclusion of multiple vegetation zones (Blarquez et al. 2015).

4.2. MAT accuracy and performance

In previous work, MAT has been used to quantitatively reconstruct continental-scale patterns of vegetation from remote-sensing data (Williams 2002). Here we showed that MAT can also perform well at reconstructing the genera biomass from pollen assemblages. Those biomass estimates are likely prone to certain sources of bias and inaccuracies discussed below, among which is the propagation of the errors related to the modern datasets (Beaudoin et al. 2014; Whitmore et al. 2005) and transfer functions that fall into the category of "known unknowns" in the sense of Jackson (2012). A relationship between pollen production and dispersal and the tree biomass should be nonetheless quantifiable. Some models linking pollen deposition and source areas have been used previously to reconstruct plant communities from pollen assemblages (Sugita 1994). Models that aim to reconstruct plant cover at the landscape scale from large lakes have been developed, mainly in Europe and, in particular, in Scandinavia (Gaillard et al. 2010). Yet those models are not parameterized for boreal ecosystems of North America. Here we simply accommodated for differential productivity and dispersal of the different taxa by using different-sized windows for assessing current vegetation based on empirical relationships. However, pollen productivity is controlled by climate (Hicks 1999), and in some cases, increasing tree density can reduce pollen production (Broström et al. 2008). However, in the absence of strictly independent proxies for climate, vegetation biomass, and pollen in the past, it is difficult to assess the relative effect of climate on pollen production. Here, because we used an analogue approach based on the principle of uniformitarianism, we must therefore assume that the relationships observed in the present such as the relationship between a pollen assemblage and the plant biomass hold in the past. This constitutes a limitation of our approach, especially because carbon allocation strategies may have changed in response to climatic and (or) disturbance events, thus modifying the relationship between pollen production and plant biomass. This relationship is thus not necessarily constant in time; however, MAT involved comparing the whole pollen assemblage typology with biomass, not that of a single taxon, likely smoothing this production bias. We also guarded against reconstructing unrealistic biomass values by carefully screening for no analogues using the ROC curve approach (Gavin et al. 2003). These no-analogue samples were numerous during the Late Glacial (14 000 – 10 000 BP; Fig. 4), a period in which no-analogue climates and plant communities are known to be widespread (Williams and Jackson 2007).

We tried to limit taphonomic issues by using only lacustrine environments from the modern dataset used to produce the transfer functions (Whitmore et al. 2005). Nevertheless, we did not consider the age of the samples in the modern database, and in a few instances, recent land use modifications may have affected the relationship between old (>50 years, ca. 1960) modern pollen samples and current remotely sensed vegetation. However, the large search radius for current biomass (>15 km) should limit uncertainties related to land cover changes that occurred during the last 50 years.

The biomass gradient used for the MAT is not even, with slightly more samples in the lower part of the biomass gradient (Fig. 3), which may result in biased RMSEP and a lower accuracy of the MAT at reconstructing high biomass values (Telford and Birks 2011). However, we showed that the MAT has a general tendency

to underestimate high biomass values, so our reconstructions should be regarded as minimal biomass estimates, and it cannot be excluded that higher biomass has occurred in the past. Because MAT is known to be sensitive to autocorrelation and to the spatial structure of the data (Guiot and De Vernal 2011; Telford and Birks 2009), we tested parametric weighted averaging transfer functions (results not shown; Simpson 2007). Nonetheless, these functions proved to be unable to reconstruct past biomass because they tended to extrapolate biomass at values below zero (Birks et al. 2010), which is nonsensical for biomass. Contrary, MAT reconstructed values were, by definition, bounded by the modern biomass dataset range, avoiding negative biomass but limiting the reconstruction to the highest current values. That being said, the question remains on the use of the MAT technique itself (Birks et al. 2010; Telford and Birks 2009) and of transfer functions based on modern samples from environments potentially impacted by human activities (Anderson 2014). Our reconstructions indeed are inherently dependent on the quality of the modern datasets (Beaudoin et al. 2014; Whitmore et al. 2005), and we showed that uncertainties could be high notably in areas impacted by human activities (Supplementary Fig. S1[1]). Thus, more studies using modern relationships and experiments that aim to constrain pollen source area in North America and to quantify pollen production bias are clearly needed.

5. Conclusion

We provided here a quantitative estimate of the tree biomass for the six main tree genera of the eastern Canadian ecosystems over the last 14 000 years. This study complements previous quantitative estimates of Quaternary forest tree cover and biome reconstructions from pollen percentages mapping (Williams 2002; Williams et al. 2004). In particular, we were able to provide past biomass estimates for genera (e.g., *Abies* and *Populus*) whose pollen is generally under-represented in sediments and whose abundance is difficult to estimate at the landscape scale. Our reconstructions indicate that the region supported at least 12 Pg of tree biomass within the eastern Canadian forest ecosystems, a value that was attained 7000 years ago concomitantly with the final collapse of the Laurentide Ice Sheet and in agreement with previous estimates (Fig. 6; Williams et al. 2011). The total biomass trend followed the deglaciation of the region and saturated rapidly within the region. Trees were probably able to survive in a periglacial environment at the ice margin and then expand from there, explaining why trees migrated so quickly and biomass saturated so rapidly (Feurdean et al. 2013), with notably biotic velocities that exceeded climatic ones at the northern fringe of postglacial tree migration (Ordonez and Williams 2013).

The mean total genera biomass was maximal only during the HTM, when higher than present insolation, higher CO_2 levels than during the LGM, and temperature and precipitation close to present-day levels favored higher tree biomass, notably for hardwood species. Interestingly, this period that corresponds to major climatic and biotic rearrangements in the region, has been shown to support higher than present biodiversity within the boreal region (including α, β, and γ diversity; Blarquez et al. 2014*a*). This could indicate that the biodiversity and biomass drivers were similar. Although it has been shown that climatic conditions likely explain both (this study; Shuman et al. 2005), the limited tree competition immediately after the deglaciation and the young stand ages at the landscape scale may also explain the elevated biomass accumulation (Ma et al. 2012). Contrarily, after the initial ice retreat and the HTM period, the ecosystems have matured, soils were formed, the biogeochemical cycles tended to become more complex, and the interactions between species were more strongly consolidated, likely restricting both tree biomass production and diversity (Blarquez et al. 2014*a*). Future conditions would probably not have analogues in the past, and the conditions that will prevail in the future (human impact, CO_2 concentration, climate, disturbances) may be well beyond past conditions. However, the results of this study can be used to estimate past carbon stocks and fluxes or to infer the mechanisms linking biomass to climate and the range within which tree communities were resilient to environmental changes. Finally, quantified past biomass estimates should be useful for assessing the role of land cover on regional climate forcing (Strandberg et al. 2014) or to test and validate hypotheses using dynamic vegetation modelling.

Acknowledgements

Data were obtained from the Neotoma Paleoecology Database (http://www.neotomadb.org), the North American Surface Sample Dataset (http://www.geography.wisc.edu/faculty/williams/lab/Downloads.html), and the Global Charcoal Database (http://paleofire.org), and the work of the data contributors and the community is gratefully acknowledged. We thank two anonymous reviewers for comments that greatly improved the quality of this manuscript.

References

Andersen, K.K., Azuma, N., Barnola, J.M., Bigler, M., Biscaye, P., Caillon, N., Chappellaz, J., Clausen, H.B., Dahl-Jensen, D., and Fischer, H. 2004. High-resolution record of Northern Hemisphere climate extending into the last interglacial period. Nature, **431**(7005): 147–151. doi:10.1038/nature02805.

Anderson, N.J. 2014. Landscape disturbance and lake response: temporal and spatial perspectives. Freshw. Rev. **7**(2): 77–120. doi:10.1608/FRJ-7.2.811.

Asnong, H., and Richard, P.J. 2003. La végétation et le climat postglaciaires du centre et de l'est de la Gaspésie, au Québec. Géogr. Phys. Quat. **57**(1): 37–63. doi: 10.7202/010330ar.

Beaudoin, A., Bernier, P.Y., Guindon, L., Villemaire, P., Guo, X., Stinson, G., Bergeron, T., Magnussen, S., and Hall, R.J. 2014. Mapping attributes of Canada's forests at moderate resolution through *k*NN imputation and modis imagery. Can. J. For. Res. **44**(5): 521–532. doi:10.1139/cjfr-2013-0401.

Bélanger, N., Carcaillet, C., Padbury, G., Harvey-Schafer, A., and Van Rees, K. 2014. Periglacial fires and trees in a continental setting of Central Canada, Upper Pleistocene. Geobiology, **12**(2): 109–118. doi:10.1111/gbi.12076.

Berger, A., and Loutre, M.F. 1991. Insolation values for the climate of the last 10 million years. Quat. Sci. Rev. **10**(4): 297–317. doi:10.1016/0277-3791(91)90033-Q.

Bergeron, Y., Gauthier, S., Flannigan, M., and Kafka, V. 2004. Fire regimes at the transition between mixedwood and coniferous boreal forest in northwestern Quebec. Ecology, **85**(7): 1916–1932. doi:10.1890/02-0716.

Birks, H.B., Heiri, O., Seppä, H., and Bjune, A.E. 2010. Strengths and weaknesses of quantitative climate reconstructions based on Late-Quaternary biological proxies. Open Ecol. J. **3**: 68–110. doi:10.2174/1874213001003020068.

Blarquez, O., and Carcaillet, C. 2010. Fire, fuel composition and resilience threshold in subalpine ecosystem. PLoS One, **5**(8): e12480. doi:10.1371/journal.pone.0012480.

Blarquez, O., Carcaillet, C., Elzein, T.M., and Roiron, P. 2012. Needle accumulation rate model-based reconstruction of palaeo-tree biomass in the western subalpine Alps. Holocene, **22**(5): 579–587. doi:10.1177/0959683611427333.

Blarquez, O., Carcaillet, C., Frejaville, T., and Bergeron, Y. 2014*a*. Disentangling the trajectories of alpha, beta and gamma plant diversity of North American boreal ecoregions since 15,500 years. Front. Ecol. Evol. **2**(6): 1–8. doi: 10.3389/fevo.2014.00006.

Blarquez, O., Vannière, B., Marlon, J.R., Daniau, A.L., Power, M.J., Brewer, S., and Bartlein, P.J. 2014*b*. paleofire: an R package to analyse sedimentary charcoal records from the Global Charcoal Database to reconstruct past biomass burning. Comput. Geosci. **72**: 255–261. doi:10.1016/j.cageo.2014.07.020.

Blarquez, O., Ali, A.A., Girardin, M.P., Grondin, P., Fréchette, B., Bergeron, Y., and Hély, C. 2015. Regional paleofire regimes affected by non-uniform climate, vegetation and human drivers. Sci. Rep. **5**: 13356 EP. doi:10.1038/srep13356.

Blois, J.L., Williams, J.W.J., Grimm, E.C., Jackson, S.T., and Graham, R.W. 2011. A methodological framework for assessing and reducing temporal uncertainty in paleovegetation mapping from late-Quaternary pollen records. Quat. Sci. Rev. **30**(15): 1926–1939. doi:10.1016/j.quascirev.2011.04.017.

Botkin, D.B., and Simpson, L.G. 1990. Biomass of the North American boreal forest: a step toward accurate global measures. Biogeochemistry, **9**: 161–174.

Bradshaw, C.J., Warkentin, I.G., and Sodhi, N.S. 2009. Urgent preservation of boreal carbon stocks and biodiversity. Trends Ecol. Evol. **24**(10): 541–548. doi:10.1016/j.tree.2009.03.019.

Bradshaw, R., and Webb, T., III. 1985. Relationships between contemporary pollen and vegetation data from Wisconsin and Michigan, USA. Ecology, **66**(3): 721–737. doi:10.2307/1940533.

Broström, A., Nielsen, A.B., Gaillard, M.-J., Hjelle, K., Mazier, F., Binney, H., Bunting, J., Fyfe, R., Meltsov, V., Poska, A., Räsänen, S., Soepboer, W., von Stedingk, H., Suutari, H., and Sugita, S. 2008. Pollen productivity estimates of key European plant taxa for quantitative reconstruction of past

vegetation: a review. Vegetation History and Archaeobotany, **17**(5): 461–478. doi:10.1007/s00334-008-0148-8.

Brubaker, L.B., Anderson, P.M., Edwards, M.E., and Lozhkin, A.V. 2005. Beringia as a glacial refugium for boreal trees and shrubs: new perspectives from mapped pollen data. J. Biogeogr. **32**(5): 833–848. doi:10.1111/j.1365-2699.2004.01203.x.

Caccianiga, M., and Payette, S. 2006. Recent advance of white spruce (*Picea glauca*) in the coastal tundra of the eastern shore of Hudson Bay (Québec, Canada). J. Biogeogr. **33**(12): 2120–2135. doi:10.1111/j.1365-2699.2006.01563.x.

Carcaillet, C., Bergeron, Y., Richard, P.J.H., Frechette, B., Gauthier, S., and Prairie, Y.T. 2001. Change of fire frequency in the eastern Canadian boreal forests during the Holocene: does vegetation composition or climate trigger the fire regime? J. Ecol. **89**(6): 930–946. doi:10.1111/j.1365-2745.2001.00614.x.

Carcaillet, C., Almquist, H., Asnong, H., Bradshaw, R., Carrion, J., Gaillard, M., Gajewski, K., Haas, J., Haberle, S., and Hadorn, P. 2002. Holocene biomass burning and global dynamics of the carbon cycle. Chemosphere, **49**(8): 845–863. doi:10.1016/S0045-6535(02)00385-5.

Comtois, P., and Payette, S. 1984. Représentation pollinique actuelle et subactuelle des peuplieraies boréales au Nouveau-Québec. Geogr. Phys. Quat. **38**(2): 123–133. doi:10.7202/032547ar.

Dale, V.H., Joyce, L.A., McNulty, S., Neilson, R.P., Ayres, M.P., Flannigan, M.D., Hanson, P.J., Irland, L.C., Lugo, A.E., Peterson, C.J., Simberloff, D., Swanson, F.J., Stocks, B.J., and Wotton, B.M. 2001. Climate change and forest disturbances. BioScience, **51**: 723–734. doi:10.1641/0006-3568(2001)051[0723:CCAFD]2.0.CO;2.

Daniau, A.L., Bartlein, P.J., Harrison, S.P., Prentice, I.C., Brewer, S., Friedlingstein, P., Harrison-Prentice, T.I., Inoue, J., Izumi, K., Marlon, J.R., Mooney, S., Power, M.J., Stevenson, J., Tinner, W., Andri, M., Atanassova, J., Behling, H., Black, M., Blarquez, O., Brown, K.J., Carcaillet, C., Colhoun, E.A., Colombaroli, D., Davis, B.A.S., D'Costa, D., Dodson, J., Dupont, L., Eshetu, Z., Gavin, D.G., Genries, A., Haberle, S., Hallett, D.J., Hope, G., Horn, S.P., Kassa, T.G., Katamura, F., Kennedy, L.M., Kershaw, P., Krivonogov, S., Long, C., Magri, D., Marinova, E., McKenzie, G.M., Moreno, P.I., Moss, P., Neumann, F.H., Norström, E., Paitre, C., Rius, D., Roberts, N., Robinson, G.S., Sasaki, N., Scott, L., Takahara, H., Terwilliger, V., Thevenon, F., Turner, R., Valsecchi, V.G., Vannière, B., Walsh, M., Williams, N., and Zhang, Y. 2012. Predictability of biomass burning in response to climate changes. Glob. Biogeochem. Cycles, **26**(4): GB4007. doi:10.1029/2011GB004249.

Dyke, A. 2004. An outline of North American deglaciation with emphasis on central and northern Canada. Developments in Quaternary Science, **2**: 373–424. doi:10.1016/S1571-0866(04)80209-4.

Feurdean, A., Bhagwat, S.A., Willis, K.J., Birks, H.J.B., Lischke, H., and Hickler, T. 2013. Tree migration-rates: narrowing the gap between inferred post-glacial rates and projected rates. PLoS One, **8**(8): e71797. doi:10.1371/journal.pone.0071797.

Flannigan, M., Logan, K., Amiro, B., Skinner, W., and Stocks, B. 2005. Future area burned in Canada. Clim. Change, **72**(1): 1–16. doi:10.1007/s10584-005-5935-y.

Fuller, J.L. 1997. Holocene forest dynamics in southern Ontario, Canada: fine-resolution pollen data. Can. J. Bot. **75**(10): 1714–1727. doi:10.1139/b97-886.

Gaillard, M.-J., Sugita, S., Mazier, F., Trondman, A.-K., Broström, A., Hickler, T., Kaplan, J.O., Kjellström, E., Kokfelt, U., Kuneš, P., Lemmen, C., Miller, P., Olofsson, J., Poska, A., Rundgren, M., Smith, B., Strandberg, G., Fyfe, R., Nielsen, A.B., Alenius, T., Balakauskas, L., Barnekow, L., Birks, H.J.B., Bjune, A., Björkman, L., Giesecke, T., Hjelle, K., Kalnina, L., Kangur, M., van der Knaap, W.O., Koff, T., Lageräs, P., Lataùowa, M., Leydet, M., Lechterbeck, J., Lindbladh, M., Odgaard, B., Peglar, S., Segerström, U., von Stedingk, H., and Seppä, H. 2010. Holocene land-cover reconstructions for studies on land cover–climate feedbacks. Clim. Past, **6**: 483–499. doi:10.5194/cp-6-483-2010.

Gauthier, S., Bernier, P., Kuuluvainen, T., Shvidenko, A., and Schepaschenko, D. 2015. Boreal forest health and global change. Science, **349**(6250): 819–822. doi:10.1126/science.aaa9092.

Gavin, D.G., Oswald, W.W., Wahl, E.R., and Williams, J.W. 2003. A statistical approach to evaluating distance metrics and analog assignments for pollen records. Quat. Res. **60**(3): 356–367. doi:10.1016/S0033-5894(03)00088-7.

Gerhart, L.M., and Ward, J.K. 2010. Plant responses to low CO_2 of the past. New Phytol. **188**(3): 674–695. doi:10.1111/j.1469-8137.2010.03441.x.

Gewehr, S., Drobyshev, I., Berninger, F., and Bergeron, Y. 2014. Soil characteristics mediate the distribution and response of boreal trees to climatic variability. Can. J. For. Res. **44**(5): 487–498. doi:10.1139/cjfr-2013-0481.

Girardin, M.P., Ali, A.A., Carcaillet, C., Blarquez, O., Hély, C., Terrier, A., Genries, A., and Bergeron, Y. 2013. Vegetation limits the impact of a warm climate on boreal wildfires. New Phytol. **199**: 1001–1011. doi:10.1111/nph.12322.

Grimm, E.C. 2008. Neotoma, an ecosystem database for the Pliocene, Pleistocene, and Holocene. Illinois State Museum Scientific Papers, E Series 1.

Grimm, E., Bradshaw, R., Brewer, S., Flantua, S., Giesecke, T., Lézine, A.-M., Willliams, J.W., and Takahara, H. 2013. Databases and their application. *In* The Encyclopedia of Quaternary Science. pp. 831–838.

Guiot, J., and De Vernal, A. 2011. Is spatial autocorrelation introducing biases in the apparent accuracy of paleoclimatic reconstructions? Quat. Sci. Rev. **30**(15): 1965–1972. doi:10.1016/j.quascirev.2011.04.022.

Hicke, J.A., Allen, C.D., Desai, A.R., Dietze, M.C., Hall, R.J., Hogg, E.H., Kashian, D.M., Moore, D., Raffa, K.F., Sturrock, R.N., and Vogelmann, J. 2012. Effects of biotic disturbances on forest carbon cycling in the United States and Canada. Glob. Chang. Biol. **18**(1): 7–34. doi:10.1111/j.1365-2486.2011.02543.x.

Hicks, S. 1999. The relationship between climate and annual pollen deposition at northern tree-lines. Chemosphere Global Change Sci. **1**(4): 403–416. doi:10.1016/S1465-9972(99)00043-4.

Higuera, P.E., Brubaker, L.B., Anderson, P.M., Hu, F.S., and Brown, T.A. 2009. Vegetation mediated the impacts of postglacial climate change on fire regimes in the south-central Brooks Range, Alaska. Ecol. Monogr. **79**(2): 201–219. doi:10.1890/07-2019.1.

Jackson, S.T. 2012. Representation of flora and vegetation in Quaternary fossil assemblages: known and unknown knowns and unknowns. Quat. Sci. Rev. **49**: 1–15. doi:10.1016/j.quascirev.2012.05.020.

Jackson, S.T., Overpeck, J.T., Webb, T., Keattch, S.E., and Anderson, K.H. 1997. Mapped plant-macrofossil and pollen records of late quaternary vegetation change in eastern North America. Quat. Sci. Rev. **16**(1): 1–70. doi:10.1016/S0277-3791(96)00047-9.

Johnson, E. 1992. Fire and vegetation dynamics: studies from the North American boreal forest. Cambridge University Press, Cambridge, UK.

Kaufman, D., Ager, T., Anderson, N., Anderson, P., Andrews, J., Bartlein, P., Brubaker, L., Coats, L., Cwynar, L., and Duvall, M. 2004. Holocene thermal maximum in the western Arctic (0–180°W). Quat. Sci. Rev. **23**(5–6): 529–560. doi:10.1016/j.quascirev.2003.09.007.

Keenan, T.F., Hollinger, D.Y., Bohrer, G., Dragoni, D., Munger, J.W., Schmid, H.P., and Richardson, A.D. 2013. Increase in forest water-use efficiency as atmospheric carbon dioxide concentrations rise. Nature, **499**(7458): 324–327. doi:10.1038/nature12291.

Kullman, L. 2002. Boreal tree taxa in the central Scandes during the Late-Glacial: implications for Late-Quaternary forest history. J. Biogeogr. **29**(9): 1117–1124. doi:10.1046/j.1365-2699.2002.00743.x.

Liu, K. 1990. Holocene paleoecology of the boreal forest and Great Lakes – St. Lawrence forest in northern Ontario. Ecol. Monogr. **62**(2): 179–212.

Liu, Z., Otto-Bliesner, B., He, F., Brady, E.C., Tomas, R., Clark, P.U., Carlson, A.E., Lynch-Stieglitz, J., Curry, W., Brook, E., Erickson, D., Jacob, R., Kutzbach, J., and Cheng, J. 2009. Transient simulation of last deglaciation with a new mechanism for Bølling–Allerød warming. Science, **325**(5938): 310–314. doi:10.1126/science.1171041.

Loarie, S.R., Duffy, P.B., Hamilton, H., Asner, G.P., Field, C.B., and Ackerly, D.D. 2009. The velocity of climate change. Nature, **462**(7276): 1052–1055. doi:10.1038/nature08649.

Ma, Z., Peng, C., Zhu, Q., Chen, H., Yu, G., Li, W., Zhou, X., Wang, W., and Zhang, W. 2012. Regional drought-induced reduction in the biomass carbon sink of Canada's boreal forests. Proc. Natl. Acad. Sci. U.S.A. **109**(7): 2423–2427. doi:10.1073/pnas.1111576109.

Mack, M.C., Bret-Harte, M.S., Hollingsworth, T.N., Jandt, R.R., Schuur, E.A., Shaver, G.R., and Verbyla, D.L. 2011. Carbon loss from an unprecedented Arctic tundra wildfire. Nature, **475**(7357): 489–492. doi:10.1038/nature10283.

Marlon, J.R., Bartlein, P.J., Daniau, A.L., Harrison, S.P., Maezumi, S.Y., Power, M.J., Tinner, W., and Vanniére, B. 2013. Global biomass burning: a synthesis and review of Holocene paleofire records and their controls. Quat. Sci. Rev. **65**: 5–25. doi:10.1016/j.quascirev.2012.11.029.

Marquer, L., Gaillard, M.-J., Sugita, S., Trondman, A.-K., Mazier, F., Nielsen, A.B., Fyfe, R.M., Vad Odgaard, B., Alenius, T., Birks, H.J.B., Bjune, A.E., Christiansen, J., Dodson, J., Edwards, K.J., Giesecke, T., Herzschuh, U., Kangur, M., Lorenz, S., Poska, A., Schult, M., and Seppä, H. 2014. Holocene changes in vegetation composition in northern Europe: why quantitative pollen-based vegetation reconstructions matter. Quat. Sci. Rev. **90**: 199–216. doi:10.1016/j.quascirev.2014.02.013.

Monnin, E., Steig, E.J., Siegenthaler, U., Kawamura, K., Schwander, J., Stauffer, B., Stocker, T.F., Morse, D.L., Barnola, J.-M., Bellier, B., Raynaud, D., and Fischer, H. 2004. Evidence for substantial accumulation rate variability in Antarctica during the Holocene, through synchronization of CO_2 in the Taylor Dome, Dome C and DML ice cores. Earth Planet. Sci. Lett. **224**(1): 45–54. doi:10.1016/j.epsl.2004.05.007.

Mousseau, M., and Saugier, B. 1992. The direct effect of increased CO_2 on gas exchange and growth of forest tree species. J. Exp. Bot. **43**(8): 1121–1130. doi:10.1093/jxb/43.8.1121.

Muller, S.D., and Richard, P.J. 2001. Post-glacial vegetation migration in conterminous Montréal Lowlands, southern Québec. J. Biogeogr. **28**(10): 1169–1193. doi:10.1046/j.1365-2699.2001.00625.x.

Ordonez, A., and Williams, J.W. 2013. Climatic and biotic velocities for woody taxa distributions over the last 16 000 years in eastern North America. Ecol. Lett. **16**(6): 773–781. doi:10.1111/ele.12110.

Overpeck, J., and Webb, T. 1985. Quantitative interpretation of fossil pollen spectra: dissimilarity coefficients and the method of modern analogs. Quat. Res. **23**(1): 87–108. doi:10.1016/0033-5894(85)90074-2.

Power, M., Marlon, J., Ortiz, N., Bartlein, P., Harrison, S., Mayle, F., Ballouche, A., Bradshaw, R., Carcaillet, C., Cordova, C., Mooney, S., Moreno, P., Prentice, I., Thonicke, K., Tinner, W., Whitlock, C., Zhang, Y., Zhao, Y., Ali, A., Anderson, R., Beer, R., Behling, H., Briles, C., Brown, K., Brunelle, A., Bush, M., Camill, P., Chu, G., Clark, J., Colombaroli, D., Connor, S., Daniau, A.L., Daniels, M., Dodson, J., Doughty, E., Edwards, M., Finsinger, W., Foster, D., Frechette, J., Gaillard, M.J., Gavin, D., Gobet, E., Haberle, S., Hallett, D.,

Higuera, P., Hope, G., Horn, S., Inoue, J., Kaltenrieder, P., Kennedy, L., Kong, Z., Larsen, C., Long, C., Lynch, J., Lynch, E., McGlone, M., Meeks, S., Mensing, S., Meyer, G., Minckley, T., Mohr, J., Nelson, D., New, J., Newnham, R., Noti, R., Oswald, W., Pierce, J., Richard, P., Rowe, C., Sanchez, Goñi, M., Shuman, B., Takahara, H., Toney, J., Turney, C., Urrego-Sanchez, D., Umbanhowar, C., Vandergoes, M., Vanniere, B., Vescovi, E., Walsh, M., Wang, X., Williams, N., Wilmshurst, J., and Zhang, J. 2008. Changes in fire regimes since the Last Glacial Maximum: an assessment based on a global synthesis and analysis of charcoal data. Clim. Dyn. **30**(7): 887–907. doi:10.1007/s00382-007-0334-x.

Ramankutty, N., and Foley, J.A. 1999. Estimating historical changes in global land cover: croplands from 1700 to 1992. Glob. Biogeochem. Cycles, **13**(4): 997–1027. doi:10.1029/1999GB900046.

Ranson, K.J., Sun, G., Lang, R.H., Chauhan, N.S., Cacciola, R.J., and Kilic, O. 1997. Mapping of boreal forest biomass from spaceborne synthetic aperture radar. J. Geophys. Res. **102**(D24): 29599–29610. doi:10.1029/96JD03708.

Reimer, P.J., Bard, E., Bayliss, A., Beck, J.W., Blackwell, P.G., Ramsey, C.B., Buck, C.E., Cheng, H., Edwards, R.L., Friedrich, M., Grootes, P.M., Guilderson, T.P., Haflidason, H., Hajdas, I., Hatté, C., Heaton, T.J., Hoffmann, D.L., Hogg, A.G., Hughen, K.A., Kaiser, K.F., Kromer, B., Manning, S.W., Niu, M., Reimer, R.W., Richards, D.A., Scott, E.M., Southon, J.R., Staff, R.A., Turney, C.S.M., and van der Plicht, J. 2013. IntCal13 and Marine13 radiocarbon age calibration curves 0–50,000 years cal BP. Radiocarbon, **55**(4): 1869–1887. doi:10.2458/azu_js_rc.55.16947.

Rhemtulla, J.M., Mladenoff, D.J., and Clayton, M.K. 2009. Historical forest baselines reveal potential for continued carbon sequestration. Proc. Natl. Acad. Sci. U.S.A. **106**(15): 6082–6087. doi:10.1073/pnas.0810076106.

Richard, P.J., Larouche, A., and Bouchard, M.A. 1982. Âge de la déglaciation finale et histoire postglaciaire de la végétation dans la partie centrale du Nouveau-Québec. Géogr. Phys. Quat. **36**(1–2): 63–90. doi:10.7202/032470ar.

Ritchie, J.C. 2004. Post-glacial vegetation of Canada. Cambridge University Press, Cambridge, UK.

Schuur, E.A., Vogel, J.G., Crummer, K.G., Lee, H., Sickman, J.O., and Osterkamp, T.E. 2009. The effect of permafrost thaw on old carbon release and net carbon exchange from tundra. Nature, **459**(7246): 556–559. doi:10.1038/nature08031.

Seppä, H., Alenius, T., Muukkonen, P., Giesecke, T., Miller, P.A., and Ojala, A.E.K. 2009. Calibrated pollen accumulation rates as a basis for quantitative tree biomass reconstructions. Holocene, **19**(2): 209–220. doi:10.1177/0959683608100565.

Shuman, B., Bartlein, P.J., and Webb, T., III. 2005. The magnitudes of millennial- and orbital-scale climatic change in eastern North America during the Late Quaternary. Quat. Sci. Rev. **24**(20–21): 2194–2206. doi:10.1016/j.quascirev.2005.03.018.

Simpson, G.L. 2007. Analogue methods in palaeoecology: using the analogue package. J. Stat. Soft. **22**: 1–29. doi:10.18637/jss.v022.i02.

Singarayer, J., and Valdes, P. 2010. High-latitude climate sensitivity to ice-sheet forcing over the last 120 kyr. Quat. Sci. Rev. **29**(1–2): 43–55. doi:10.1016/j.quascirev.2009.10.011.

Strandberg, G., Kjellström, E., Poska, A., Wagner, S., Gaillard, M.-J., Trondman, A.-K., Mauri, A., Davis, B.A.S., Kaplan, J.O., Birks, H.J.B, Bjune, A.E., Fyfe, R., Giesecke, T., Kalnina, L., Kangur, M., van der Knaap, W.O., Kokfelt, U., Kuneš, P., Latalowa, M., Marquer, L., Mazier, F., Nielsen, A.B., Smith, B., Seppä, H., and Sugita, S. 2014. Regional climate model simulations for Europe at 6 and 0.2 k BP: sensitivity to changes in anthropogenic deforestation. Clim. Past, **10**(2): 661–680. doi:10.5194/cp-10-661-2014.

Sugita, S. 1994. Pollen representation of vegetation in Quaternary sediments: theory and method in patchy vegetation. J. Ecol. **82**(4): 881–897. doi:10.2307/2261452.

Telford, R., and Birks, H. 2009. Evaluation of transfer functions in spatially structured environments. Quat. Sci. Rev. **28**(13): 1309–1316. doi:10.1016/j.quascirev.2008.12.020.

Telford, R.J., and Birks, H.J.B. 2011. Effect of uneven sampling along an environmental gradient on transfer-function performance. J. Paleolimnol. **46**(1): 99–106. doi:10.1007/s10933-011-9523-z.

Telford, R., Andersson, C., Birks, H., and Juggins, S. 2004. Biases in the estimation of transfer function prediction errors. Paleoceanography, **19**(4). doi:10.1029/2004PA001072.

Tibshirani, R. 1996. Regression shrinkage and selection via the lasso. J. R. Stat. Soc. Series B Stat. Methodol. **58**(1): 267–288.

Tjoelker, M., Oleksyn, J., and Reich, P. 1998. Seedlings of five boreal tree species differ in acclimation of net photosynthesis to elevated CO_2 and temperature. Tree Physiol. **18**(11): 715–726. doi:10.1093/treephys/18.11.715.

van Vuuren, D.P., Edmonds, J., Kainuma, M., Riahi, K., Thomson, A., Hibbard, K., Hurtt, G.C., Kram, T., Krey, V., Lamarque, J.-F., Masui, T., Meinshausen, M., Nakicenovic, N., Smith, S.J., and Rose, S.K. 2011. The representative concentration pathways: an overview. Clim. Change, **109**: 5–31. doi:10.1007/s10584-011-0148-z.

Watts, W. 1979. Late Quaternary vegetation of central Appalachia and the New Jersey Coastal Plain, USA. Ecol. Monogr. **49**: 427–469. doi:10.2307/1942471.

Whitmore, J., Gajewski, K., Sawada, M., Williams, J.W., Shuman, B., Bartlein, P.J., Minckley, T., Viau, M.A.E., Webb, T., III, Shafer, S., Anderson, P., and Brubaker, L. 2005. Modern pollen data from North America and Greenland for multi-scale paleoenvironmental applications. Quat. Sci. Rev. **24**(16): 1828–1848. doi:10.1016/j.quascirev.2005.03.005.

Williams, J.W. 2002. Variations in tree cover in North America since the last glacial maximum. Glob. Planet. Change, **35**(1): 1–23. doi:10.1016/S0921-8181+(02)00088-7.

Williams, J.W., and Jackson, S.T. 2007. Novel climates, no-analog communities, and ecological surprises. Front. Ecol. Environ. **5**(9): 475–482. doi:10.1890/070037.

Williams, J., and Shuman, B. 2008. Obtaining accurate and precise environmental reconstructions from the modern analog technique and North American surface pollen dataset. Quat. Sci. Rev. **27**(7): 669–687. doi:10.1016/j.quascirev.2008.01.004.

Williams, J.W., Shuman, B.N., Webb, T., III, Bartlein, P.J., and Leduc, P.L. 2004. Late-Quaternary vegetation dynamics in North America: scaling from taxa to biomes. Ecol. Monogr. **74**(2): 309–334. doi:10.1890/02-4045.

Williams, J.W., Tarasov, P., Brewer, S., and Notaro, M. 2011. Late Quaternary variations in tree cover at the northern forest–tundra ecotone. J. Geophys. Res.: Biogeosci. **116**(G1). doi:10.1029/2010JG001458.